MoIsw2; the missing link between adaptation and mutation instrumental for natural adaptation-directed fast evolution (NADFE) of Magnaporthe oryzae

Mengtian Pei[1], Yakubu Saddeeq Abubakar[2,3], Hina Ali[1], Xianying Dou[1], Guodong Lu[1], Zonghua Wang[1,4], Ya Li[1*] Stefan Olsson[1,5*]

[1]State Key Laboratory of Ecological Pest Control for Fujian and Taiwan Crops, College of Plant Protection, Fujian Agriculture and Forestry University, Fuzhou 350002, China

[2]Key Laboratory for Plant-microbe Interaction, College of Life Sciences, Fujian Agriculture and Forestry University, Fuzhou 350002, China

[3]Department of Biochemistry, Faculty of Life Sciences, Ahmadu Bello University, Zaria, Nigeria

[4]Institute of Oceanography, Minjiang University, Fuzhou, China

[5]Plant Immunity Center, Haixia Institute of Science and Technology, College of Life Science, Fujian Agriculture and Forestry University, Fuzhou 350002, China

*Correspondence:

Ya Li and Stefan Olsson

liya-81@163.com & Stefan@olssonstefan.com

Abstract

Isw2 is known to bind DNA, using a Myb-type DNA binding domain and with another part of the protein interact with histones in the closest nucleosome to pull the two closest nucleosomes closer to the binding site using ATP. These bindings hinder these nucleosomes' sliding movements and affect histone tail modification and DNA methylation but give more space for sliding and access for transcription factors further away from the Isw2 DNA binding sites. In a previous paper, we have knocked out the *Magnaporthe oryzae* Isw2 protein and complemented it with a GFP-labelled construct. We found that the *MoISW2* is needed, especially in the later necrotrophic stages of infection when the plant starts defending itself.

Using published transcriptomic data, we have now found that *MoISW2* is mainly co-regulated with Histone 4 (*MoHIS4*), which likely indicates that MoIsw2 predominately interacts with MoHis4. We performed a ChIP-seq experiment using MoIsw2-GFP to map the binding sites and investigated if MoIsw2 regulates genes by the limited sliding type mechanism and if this regulation could be involved in pathogenicity regulation. Common motifs were found in the binding DNA sequences using MEME. Interestingly, these motifs were mainly intergenic, and a dominant palindrome motif was present in 200 sequences.

We further performed an RNAseq for *ΔMoisw2* compared with the *Ku80* background strain and used genes sorted in physical order on the supercontigs to determine the effect of the mutation on the regulation of the genes physically close to the MoIsw2 binding sites. The genes close to the binding site were more absolutely regulated in the *ΔMoisw2* mutant as expected due to the limited sliding mechaninsm. As nucleosomes are evenly distributed at roughly 200bp distance, there should be an interference pattern of regulation of genes centered around the MoIsw2 DNA binding site if the genes are roughly evenly distributed now given more space to slide due to this mechnism, which could be confirmed. We queried the NCBI database again and checked where the about 200 palindromic sequences were found in the genome to investigate if MoIsw2 binds to any known

structures in the DNA. The palindromic sequences were found in conserved retrotransposon elements that generally contain palindromes. Since these retrotransposon elements can move place, they can create new regulatory variations with MoIsw2. Many avirulence genes recognized by different host plant cultivars and typically vary in expression between pathogen isolates were close to the MoIsw2 DNA binding site. That could mean that mobile elements associated with some MoIsw2 DNA binding sites are involved in creating variations in the pathogenicity of different *M. oryzae* strains. To test this idea, we searched through the transcriptomic data of our strain (70-15) and another strain (98-05) for variation in *AVR* expression during infection and if differences in MoIsw2 binding could be the cause for this variation and it seems to be that. Finally, we found that most of the genes upregulated in the *ΔMoisw2* mutant regulate biomass growth (DNA-binding and quality control, and TFs overrepresented). In contrast, the ones downregulated have to do with mainly mitochondrial oxidative phosphorylation, oxidative stresses, and secondary metabolites. Similar results for enriched and depleted genes were found for all genes in our ChIP-seq data for genes closest to MoIsw2 binding. We conclude that MoIsw2 interaction with nucleosomes and binding to palindromic DNA in transposons located between genes creates a possibility for an evolutionary fast variation of offspring regulatory pattern without loss of genes through mutation and fast creation of *M.oryzae* strains with new cultivar host ranges in response to defenses by resistant cultivars and consequently a fast break of resistance. *MoISW2* seems to lay a mechanistic ground for natural adaptation-directed fast evolution (NADFE) of *M. oryzae*, which is discussed as a new concept for Eukaryotes.

Author contributions:

Mengtian Pie: ChIPseq and initial analyses; RNAseq and initial analyses; manuscript preparation and writing.

Yakubu Saddeq Abubakar: Constructive manuscript critique; manuscript corrections

Hina Ali: ChPseq; RNAseq

Xianying Dou: Constructive manuscript critique; manuscript corrections

Guodong Lu: Supervision; manuscript corrections

Zonghua Wang: Supervision; manuscript corrections

Ya Li: Obtaining funds; supervision; initial planning of experiments; manuscript preparation and writing

Stefan Olsson: ChIPseq and RNAseq extended analyses and synthesis; MEME, FungiFun, antiSMASH analyses; manuscript planning; manuscript preparation and writing.

Keywords: heterochromatin, epigenetics, nucleosomes, avirulence genes, retrotransposons, evolution

Introduction

The eukaryotic genome is organized into condensed nucleosomes limiting access to DNA for transcription factors and more loosely packed regions easier to access for interaction with DNA for transcription factors and repressors. The cell inheritance of this pattern is the basis of animal cell line specialization during embryogenesis (Serrano et al., 2013). Thus DNA accessibility also in fungi plays an essential role in determining which genes can be accessed to be efficiently transcribed (Huang et al., 2021).

ISW2 proteins contain a Myb/Sant domain close to their C-terminal that binds DNA. Isw2 has a histone binding domain that interacts with Histone 4 of a nucleosome and a catalytic ATPase domain that can react with ATP and change the protein (Whitehouse et al., 2007; Hota and Bartholomew, 2011; Dang et al., 2014) then the protein change conformation so that the nucleosome moves towards the DNA binding point of the ISW2 (Fazzio et al., 2005). Since this happens in both directions, it has been shown that it causes a localized nucleosome condensation (heterochromatin) that negatively affects the expression of the genes closest to the DNA-binding site (Whitehouse et al., 2007). There has been much research into this area, but it has become clear that in vitro mapping of ISW2 binding and nucleosome positioning does not reflect what happens *in vivo* (Fazzio et al., 2005; Donovan et al., 2021). In both these articles, the authors suggested that ISW2 is involved in targeted nucleosome positioning around their DNA-binding site based on their results. The nucleosomes closest to the ISW2 binding sites get locked by interacting with ISW2, whose activity keeps them close together while nucleosomes at a further distance get less condensed and nucleosomes more freedom to move. The accessibility for transcription will then be limited close to the ISW2 DNA binding site while varying with distance from it in a sinus wave pattern caused by the possibility for nucleosome movements (Donovan et al., 2021). Furthermore, ChIP seq experiments have shown that both the largest subunit of the ISW2 complex, ISW2, and Itc1, are needed for robust, target-specific binding to DNA while ISW2 is sufficient for basal level binding (Fazzio et al., 2005).

We have previously identified all Myb containing DNA binding proteins to investigate if any of them have a role in pathogenicity. We then found a MoISW2 candidate since it has an MYB/SANT domain (in our paper, the gene was named MoMyb15) that had considerable effects on the later necrotrophic stages of infection (Li et al., 2021). Especially interesting is if MoISW2 regulates pathogenicity-related genes at later stages of infection when the fungus is exposed to stresses imposed by the plant defenses and since the deletion of the gene significantly affected *M. oryzae* pathogenicity (Li et al., 2021).

We now find that the MoISW2 protein regulates gene expression consistent with regulation through epigenetics through DNA and nucleosome binding. The most upregulated genes by the MoISW2 activity are genes involved in mitochondrial, oxidative stress-related genes and the production of secondary metabolites. This ISW2 activity is also likely to help create positive mutation bias, as very recently shown to exist for genes involved in reacting to the environment (Monroe et al., 2022) in genes affected by the MoISW2 activities. Most downregulated genes favor DNA synthesis, DNA quality control needed for fast DNA synthesis, and biomass growth. Our results indicate that MoISW2 epigenetically silences avirulence genes differently in different *M. oryzae* isolates. The MoISW2 binding is commonly in retrotransposon-like DNA sequences between genes, pointing to that MoISW2 binding sites and regulation can be shifted evolutionary fast in the *M. oryzae* genome.

Results

Correlation analyses of ISW2 expression with expressions of nucleosomal histones

Histone 1 is involved in epigenetic silencing, and its expression and density are linked to the silencing activity (Willcockson et al., 2021). Isw2 binds DNA and histone 4 (Donovan et al., 2021). To investigate correlations between histones and the putative MoIsw2 for our strain, we used published expression data, from the course of rice leaf infection, from many different published experiments, as we have done previously for other genes (Zhang et al., 2019) (70-15). The *MoHIS1* expression increases steeply with *MoISW2* gene expression. The putative *MoISW2* is also found to be co-regulated with a putative *MoHIS4* in the downloaded data (**Fig. 1**). Thus, it could mean that the putative *MoISW2* (Li et al., 2021) is a true *MoISW2*. The expression of *MoHIS2B* is related to the overall growth rate (Zhang et al., 2019) and is correlated with *MoISW2,* but not with a steep slope, indicating that a smaller amount of MoHis2B is needed for the DNA synthesis per cell. Similarly, for the expression of *MoHIS3* but not for *MoHIS2A*, that are not significantly correlated with the putative *MoISW2*. **(Fig. S1).** The other histones expressions were less correlated with the putative *MoISW2* (**Fig. S1**). Isw2 works together with ITC1 and His4; thus the expression of these three putative genes should be correlated in *M. oryzae,* and they are nicely correlated in the data from plant infection (**Fig. S2**).

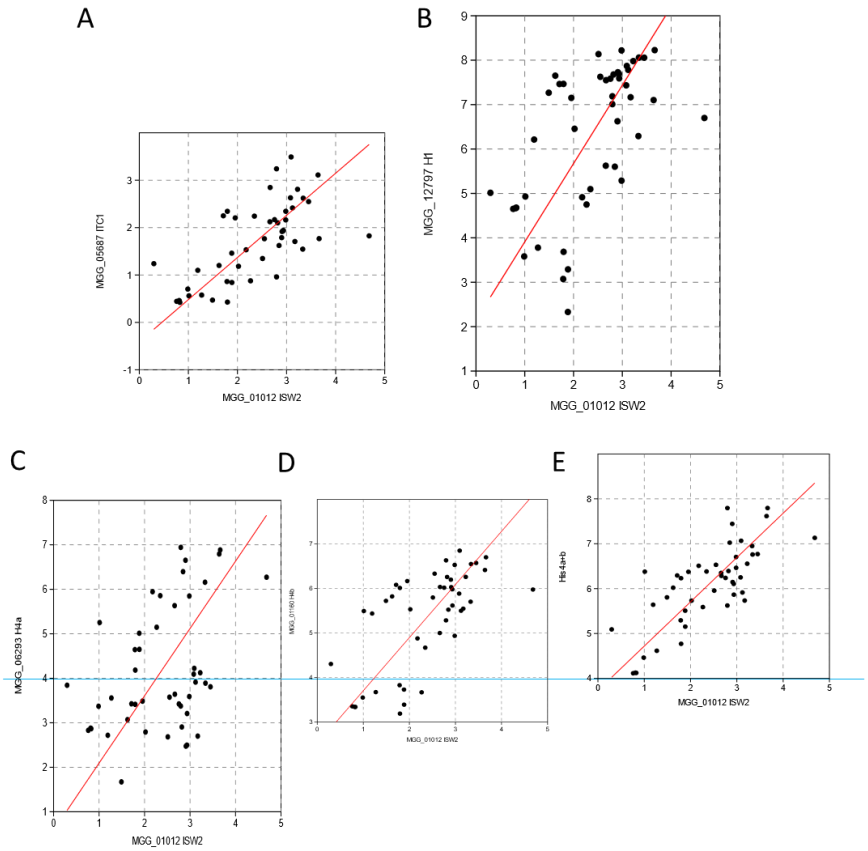

Figure 1. Log2 Reduced Major Axis (RMA) correlations of a putative ITC1, the linker histone Histone1 and the two putative histone 4 genes putatively expressing the same protein known to interact with the expression of the putative *MoISW2* (x-axis) in published RNAseq data at different stages of plant infection. Each dot

represents the two genes' expression in a separate RNAseq dataset. RMA fitting was used to handle the problem of errors in both X and Y axis values, an inherent consequence of plotting the expression of 2 genes against each other. Each dot corresponds to the value from one transcriptome. (**A**) ITC1, P(uncorr)=1.57E-7 (**B**) Histone 1, P(uncorr)=1.48E-5 (**C**) Histone 4a P(uncorr)=0.0044 (**D**) Histone 4b P(uncorr)=3.81E-7 (**E**) Histone 4a + 4b since both Histone 4 genes are predicted to encode for exactly the same protein, P(uncorr) 5.82e-10. All plots are shown with equal x and y scale gradings so that it is easy to compare slopes between graphs visually. Also, note that figures **C**, **D**, and **E** have been positioned so that Log 4 on the Y-axes are on the same line so that the effect of the addition, Log2(His4a+His4b), can be seen visually.

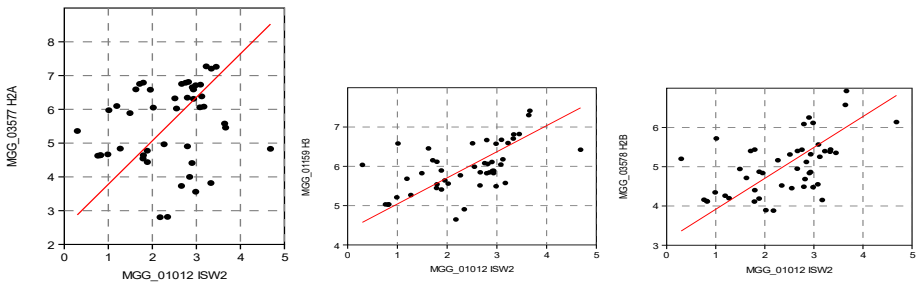

Figure S1. Log2 RMA correlations of a putative *MoHIS2a, MoHIS3* and *MoHIS2B* with expression of *MoISW2* (x-axis) in published RNAseq data at different stages of plant infection. (**A**) *MoHIS2a*, P(uncorr=0.20 (**B**) *MoHIS3*, P(uncorr)=8.94E-5 (**C**) *MoHIS2B*, P(uncorr)=3.56E-5.

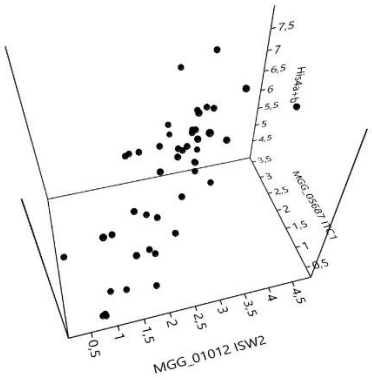

Figure S2. 3D plot showing Log of expression of *MoISW2*, *MoITC1*, and *MoHIS4a+b* that, according to the literature, need to work together to influence nucleosome packing.

Thus, the putative *MoISW2* gene likely encodes a putative MoIsw2 protein involved in targeted local chromatin compaction working with MoHis1 and MoHis4 (Fazzio et al., 2005; Donovan et al., 2021; Willcockson et al., 2021). From now on, we skip "putative" as an attribute and investigate if MoIsw2 has the expected functions as an Isw2 and what other effects it likely has on the biology of the fungus. Also, the local chromatin compaction caused by MoIsw2 should be dynamic and more decisive the more the gene and the protein are expressed.

ChIP-seq analysis to find likely intergenetic palindromic DNA binding motifs

We used a *MoISW2-GFP* construct from our previous study (Li et al., 2021) to perform a ChIP-seq analysis to find conserved DNA binding motifs for the binding of MoIsw2 to *M. oryzae* DNA sequences. We looked especially for palindromic motifs in the sequences interacting with MoIsw2-

GFP since our hits in the ChIP-seq data showed hits mainly for intergenic sequences (**Supplemental Data 1**), where transposable elements (TEs) are commonly located with TE target sites that are often palindromic (Linheiro and Bergman, 2008). In addition, TEs are involved in stress adaptation, and host specialization of *M. oryzae* (Chadha and Sharma, 2014; Yoshida et al., 2016), and our previous work showed MoIsw2 to be especially needed when plant host innate immune responses are known to be high (Li et al., 2021). In addition, interacting with a palindromic sequence that is likely to form hairpin structures in DNA (Ganapathiraju et al., 2020) can make "non-sliding" anchors for MoIsw2 to pull nucleosomes closer. We found the most common palindromic motif in 196 of our ChIP-seq DNA sequences using the MEME website, and there, the MEME search engine to search for common motifs (**Fig. 2A. Supplemental Data 2**). This motif has similarities with a staggered-cut palindromic target site involved in transposon cut and paste (Linheiro and Bergman, 2008).

Using a TOMTOM search at the MEME website, we could see that the found palindromic motif has similarities to a known Myb-binding protein containing DNA binding motif from humans (**Fig. 2B Supplemental Data 3**). The large number of palindromic hits and their alleged similarities with a human Myb since ISW2 contains a Myb-SANT domain (Li et al., 2021) made us focus on these 196 hits to investigate how and if genes are regulated around these sites in the genome to test if MoISW2 is involved in local chromatin compaction around the sites of these palindromic DNA motifs for MoISW2 DNA binding.

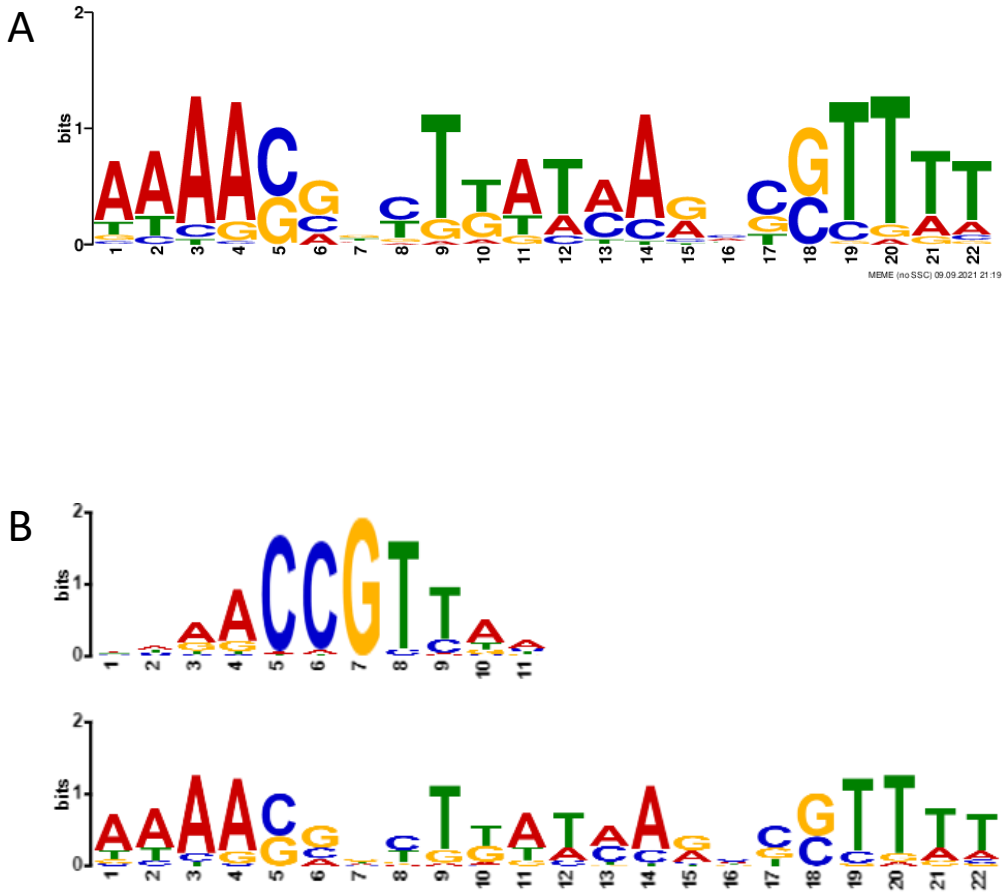

Figure 2. One common palindromic motif was found for MoIsw2 DNA binding in *M.oryzae* gene promoter regions. (**A**) The motif is found in 196 ChIP-seq sequences. (**B**) Comparison of the motif (Top) with the known human Myb protein DNA binding motif (bottom) found by TOMTOM. The ISW2 DNA binding domain is a Myb/SANT domain.

The binding of MoIsw2 regulates the genes closest to the motif binding site

We found that the196 motifs for binding sites were primarily intergenic, and we investigated the regulation of the genes closest to these 196 MoIsw2 binding sites to see if MoIsw2 restricts the regulation of the genes closest to the DNA binding site, as would be expected (Donovan et al., 2021). We searched all ChIP-seq sequences against the NCBI database and found good hits for 176 of the 196 motifs. Most of these hits were intergenic (113), while the rest (63) were in the promoter region. We next performed an RNAseq for the *ΔMoisw2* strain and the background *Ku80* strain, where we investigated the regulation of the gene with the hit in the promoter region or the closest gene to the intergenic binding site (**Fig. 3**). Only genes expressed at all in our datasets were included in the analysis. There was a general upregulation of the closest genes to the MoIsw2 binding site in the*ΔMoisw2* mutant (**Fig. 3A**). For these genes, the *ΔMoisw2* / *Ku80* expression ratio is lower when the MoIsw2 is predicted to bind directly in the promoter region than for the closest gene of a predicted intergenic binding. When the absolute (positive or negative) regulation was considered, on the other hand, both types of genes with MoIsw2 binding in the promoter had similar absolute regulation indicating that many genes with MoIsw2 binding their promoter region are repressed in *ΔMoisw2* (**Fig. 3B**). The latter supports MoIsw2 as an Isw2 protein that creates a local nucleosome condensation at specific nucleosomes (Donovan et al., 2021).

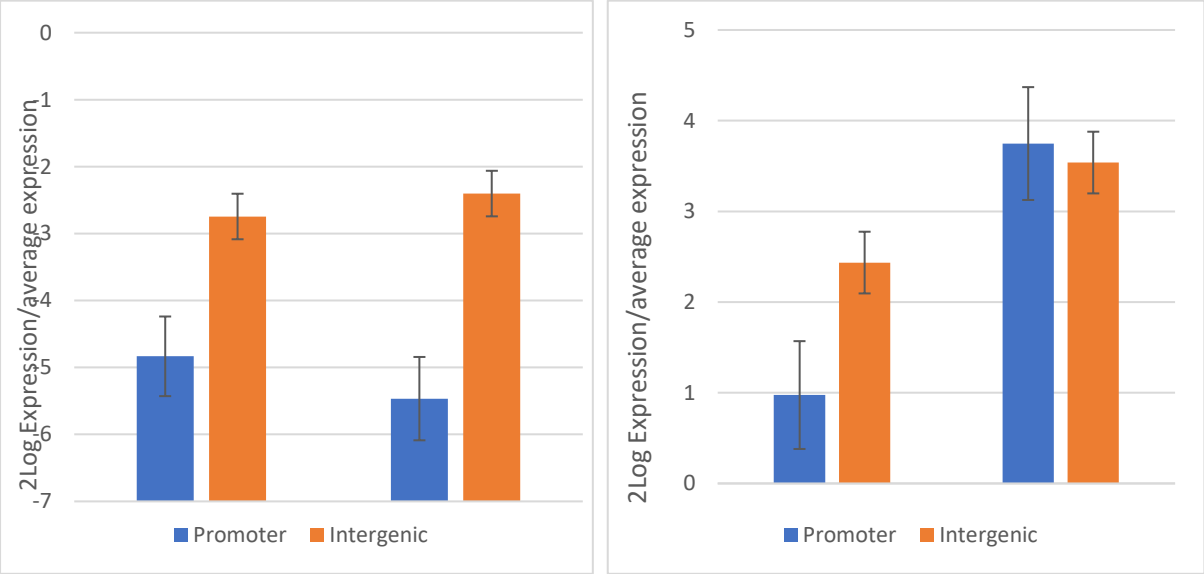

Figure 3. Regulation of genes closest to the predicted palindromic MoIsw2 binding site with hits for the MoISW2 binding in the ChIP-seq data. (**A**) Expression was on average higher in *ΔMoisw2* than *Ku80* of genes closest to the binding site or with the motif in their promoter region. (**B**) Change in expression for genes with a binding site in the promoter region and the closest gene when ISW2 is intergenic. Deleting MoISW2 upregulates both types of genes and upregulates genes more slightly further away from the binding site while the absolute (plus or minus) regulation is equal for both types of genes (8-16 times regulation). Error bars indicate SEM (Promoter N=63 Intergenic N=112).

Several genes close to the MoIsw2 binding site were neither expressed in *ΔMoisw2* nor *Ku80,* indicating that these genes could be permanently non-expressible potential pseudogenes without biological roles. We only use the term pseudogene in its limited sense (Cheetham et al., 2020) for genes that look like genes without any roles and are not expressed under many natural conditions. Since the overuse of the pseudogene term does not make sense, we follow the nomenclature suggested (Cheetham et al., 2020). Since the non-existence of a role can never be firmly tested

experimentally, we prefer to call them potential pseudogenes. Our observation that these genes are or have become potential pseudogenes during evolution is exciting since some genes are annotated as avirulence genes (**see Table 1**). The data and analyses for this and the next section is available in a supplemental file (**Supplemental Data 4**)

Local gene regulations around MoIsw2 palindromic DNA binding sites fit the Isw2 specific DNA binding model and can likely be used to estimate the NRL size around the binding site.

To further investigate local regulation around the binding sites with the found palindromic motif, we investigated our RNAseq data and ordered the MGG_codes for the genes in the order of the genes on the supercontigs (Supercontig order downloaded from BROAD). We found that genes upstream and downstream, the genes closest to the binding site (+8/-8 genes), were generally differently regulated, and *ΔMoisw2* differed from the background *Ku80* in this respect.

Because of the targeted local nucleosome condensation, the gene regulation around the Isw2 binding site (Donovan et al., 2021) *ΔMoisw2*/*W.T.* regulation should be in waves around the DNA attachment point due to the likely interference pattern (phasing) between nucleosome repeat lengths (NRLs) and the average distance between gene promoter sequences, if the average gene distance is similar for most genes (Chereji et al., 2018). We first calculated the average gene distance in *M.oryzae* using the downloaded data from BROAD and found that the average distance is 4659bp for all genes ordered on supercontigs with a relatively small standard error of 203 bp (SEM=4%). We then searched for the best fit of a sinus function of the *ΔMoisw2/Ku80* transcription using our gene expression data (RNAseq) of the +8/-8 genes surrounding the MoIsw2 binding site. We used MS Excel Solver to fit a reflecting sinus wave, reflecting with a minimum in the MoIsw2 attachment point. We used a sinus function since DNA are wrapped around and slides around nucleosomes of similar sizes, with a constant overall NRL (van Holde, 1989; Cutter and Hayes, 2015; Donovan et al., 2021; Willcockson et al., 2021) and NRLs sizes depending on the organism, cell type and cell status (van Holde, 1989). We found a general up-regulation at the point of DNA-interaction (**Fig. 3**) and waves of regulation on each side of the DNA-binding site for MoIsw2 probably due to changed nucleosome phasing affecting the *in vivo* transcription (Chereji et al., 2018) differently in *ΔMoisw2* and the background *Ku80*. By searching for the best fit with the minimum wavelength (**Fig. 4**) that can create the observed data, we could approximate that the predicted average NRLs close to the MoIsw2 DNA attachment should be 211bp with an SEM of 9bp. That roughly agrees with Donovan et al. (2021) and what could be expected for not highly condensed NRLs (van Holde, 1989).

Since Isw2 interacts with histone 4 (Donovan et al., 2021), we made a few attempts to detect MoIsw2 interaction with a putative MoHis4 protein using a yeast two-hybrid assay. We could not detect any interaction solid and long enough to give a positive result. Thus, there might be no interaction, or the interaction is very transient; the latter is likely (see discussion).

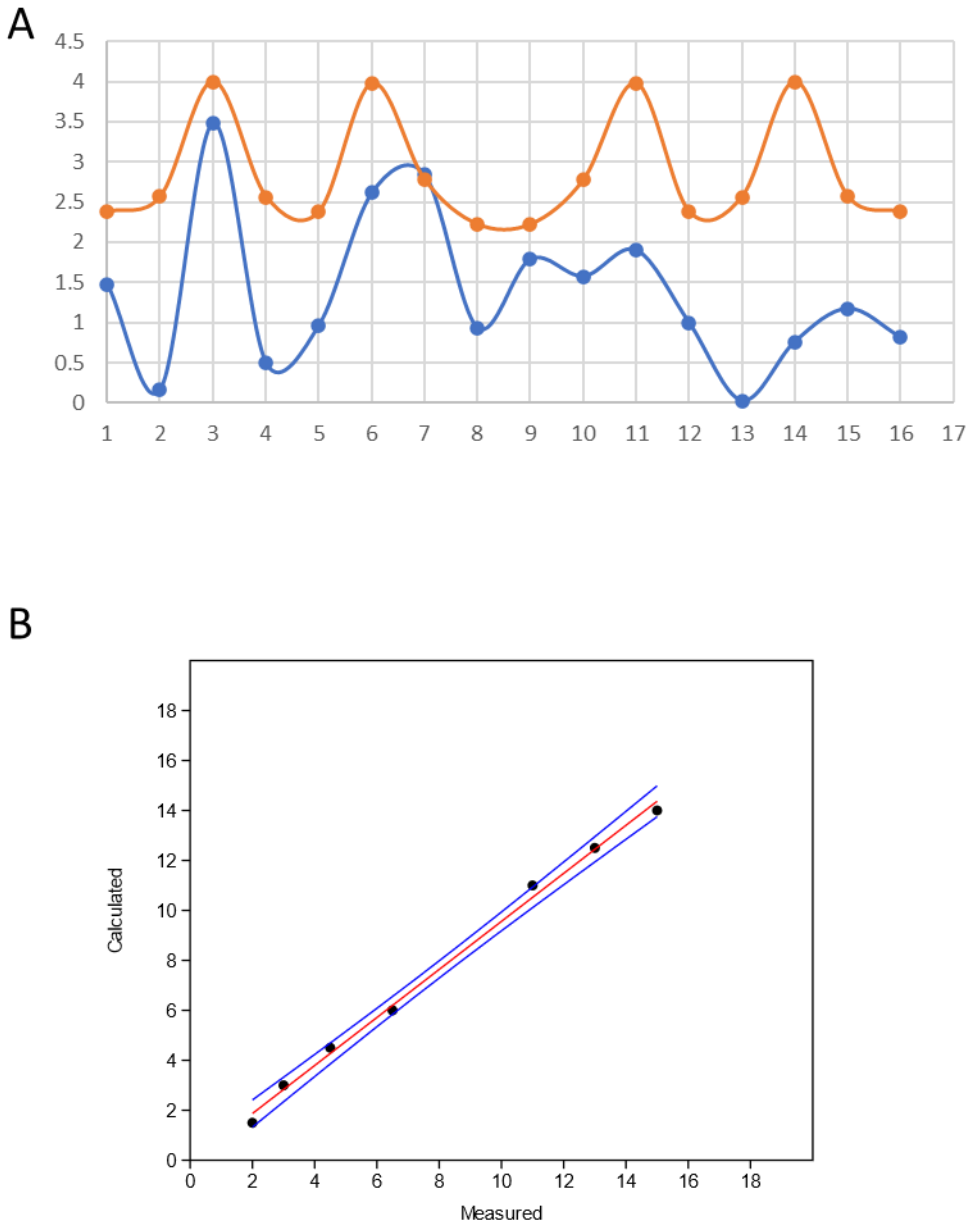

Figure 4. 2Log *ΔMoisw2* mutant/*Ku80* expression of the genes -8 to +8 genes around the palindromic MoIsw2 palindromic binding site (8.5) occurs in waves. (**A**) Fitting a sinus curve with reflection at the MoIsw2 binding sites. Regulation in general LogNormal. Using measured data blue curve with a sinus equation can be done after a Y axis offset since if the the Excel Solver function if that is set to minimize the sum of square solution for the difference between observed (blue dots) and the calculated dfom the fit (orange dots). The lines are not calculated they are the normal excel smooth-line connectors between dots(**B**). The linear regression correlates between peak and valley positions read from the two graphs in the top figure, showing that the curves are well in phase with each other. Black =Peak position Red=valley position. Blue lines (95% confidence interval for the relationship).

Palindromic sequences between genes often target transposon sequences, and MoISW2 DNA binding the palindromic DNA motif can influence close-by avirulence genes expression.

Palindromic DNA are typical mobile elements of retrotransposons. Avirulence proteins are pathogenicity-related fungal proteins that the plant senses and mounts innate immunity reactions towards. These genes are generally situated close to known retrotransposons in the *M. oryzae* genome (Yoshida et al., 2016). Most of the 196 ChIP-seq sequences with palindromic binding motifs were found in known mobile elements (transposons).

Sub-hypothesis from the above observation: If avirulence gene expressions in *M. oryzae* are affected by MoISW2 targeted nucleosome condensation, then transposable elements interacting with MoIsw2 could be directly involved in the pathogen-plant arms race between pathogen pathogenicity and plant resistance. Moreover, these genes should be adjacent to the MoIsw2 binding site, and their expression should be affected differently depending on their closeness to the binding site.

To test this hypothesis, we first made a list of all known avirulence genes noted for *M. oryzae* at NCBI (**Table 1**). We found 16 avirulence genes of different types and the avirulence cluster for cytochalasan type compound biosynthesis (Collemare et al., 2008; Song et al., 2015) containing 12 more genes. The cytochalasan cluster is specifically activated at early hours post infection HPI during penetration and produces a secondary metabolite recognized by the *R* gene *Pi33* in resistant rice cultivars (Collemare et al., 2008). Avr-PWL1 and Avr-PWL2 (Dioh et al., 2000), together with the previous, makes 18 classic avirulence type genes excluding the cytochalasan gene cluster genes (**Table 1**).

Most of the genes in the cytochalasan cluster are very close to the MoIsw2 palindromic DNA binding motif site, and several are differently expressed in 70-15 and 98-06 (**Table 1**), which might lead to the production of different final metabolites from the gene cluster even if the metabolites have similar functions as virulence factors.

Six of the other avirulence genes are not expressed in either strain (**Table 1**). Of these 6, half of the genes are close to the MoIsw2 binding site, and 3 are further away in 70-15. Two Avir genes (MGG_17614 and MGG_15611) are on supercontigs with unknown gene-order in our data, so it is unsure how far they are from a MoIsw2 binding site. The positioning of the MoIsw2 binding site close to retrotransposons and the differential regulation and expression variation make it likely that MoIsw2 specific targeting nucleosome binding is instrumental for stabilizing avirulence gene expression appropriately, concerning fungal-experienced plant host immune reactions. The data and analyses for this section is available in a supplemental file (**Supplemental Data 5**)

Table 1. Comparison of the position of avirulence genes in relation to the MoIsw2 palindromic DNA binding motif site in strain 70-15, as well as expression of the avirulence genes in MoISW2 knockout compared to the background; and expression of the same genes during infection of rice for strain 70-15 and strain 98-0 from published data. Yellow-marked cells; are genes that MoIsw2 downregulates in 70-15. Orange marked cells; genes with no expression could be potential pseudogenes in 70-15 and/or 98-0. Green marked cells; are genes that are only expressed during infection by one of the strains

ID.	Annotation	Within or outside the +8/-8 genes around the MoIsw2 binding site	More In KO (X)	Absent expression in both strains (X)	Less in KO. (X)	Only in 70-15 (X)	Only in 98-0 (X)	Expressed in both strains and in 70-15 infection data	Expression in WT 70-15 infection data
MGG_12447	cytochalasan	Within	X					X	X
MGG_08386	cytochalasan	Within		X					
MGG_08377	cytochalasan	Within	X					X	X
MGG_08378	cytochalasan	Within	X					X	X
MGG_08380	cytochalasan	Within					X		
MGG_08381	cytochalasan	Within					X		ND
MGG_08384	cytochalasan	Within	X					X	X
MGG_08389	cytochalasan	Within			X			x	X
MGG_08390	cytochalasan	Within						X	X
MGG_08391	cytochalasan	Within					X		
MGG_15927	cytochalasan	Within					X		
MGG_15928	cytochalasan	Within	X			X			
	Avirulence genes								
MGG_07199	ATR13, RxLR effector	Outside						X	X
MGG_10556	Avr_Pii	4 genes away		X					
MGG_17614	Avr_Pii	nonordered			X	X			ND
MGG_13283	Avr_Pik	Outside		X					
MGG_15972	Avr_Pik	nonordered	X					X	X
MGG_03029	Avr_Pita1	Outside			X			X	X
MGG_07038	Avr_Pita1	Outside			X			X	X
MGG_09617	Avr_Pita1	1 genes away		X					
MGG_10927	Avr_Pita1	13 genes away	X					X	X
MGG_03808	Avr_Pita1 like	Outside		X					
MGG_15370	Avr_Pita1 like	1genes away	X					X	X
MGG_17611	Avr_Pita1 middle	nonordered	X						ND
MGG_14981	AVR_PiTA2	Outside		X					
MGG_15212	AVR_Pita2	4 genes away					X		
MGG_18041	Avr_Piz-t	nonordered						X	ND
MGG_03685	Avr-Pi54	Outside	X					X	X
MGG_13863	Avr-PWL1	2genes away					X		
MGG_07398	Avr-PWL2	Outside				X			

RNA-seq data of *ΔMoisw2* and *Ku80* indicates that MoIsw2 regulates the balance between glycolytic growth with biosynthesis, and aerobic catabolism

For *ΔMoisw2* grown on MM-medium, 339 genes were significantly upregulated compared to the background *Ku80*. The two largest significantly overrepresented gene categories were for secondary metabolism and DNA-binding, while most of the other categories are related to DNA synthesis and DNA-related activities (**Fig. 5A**). These are the genes MoISW2 likely negatively regulates in *Ku80*. Most of the downregulated genes in the *ΔMoisw2* are genes involved in mitochondrial electron transport and other mitochondrial processes. In other words, our results indicate that MoIsw2 is involved in regulating the balance between DNA synthesis, which is safest without ATP generation by mitochondrial respiration that generates Radical Oxygen Species (ROS) that is a necessary biproduct of respiratory metabolism (Klevecz et al., 2004).

A

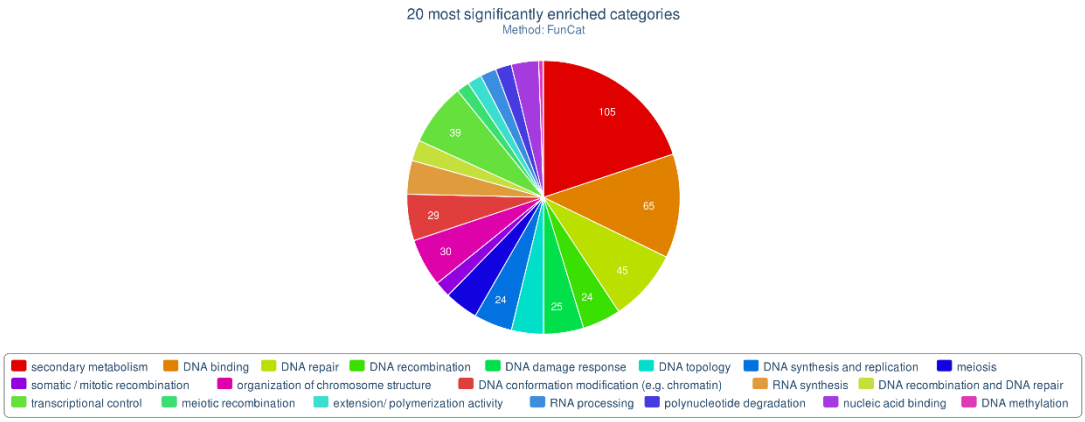

B

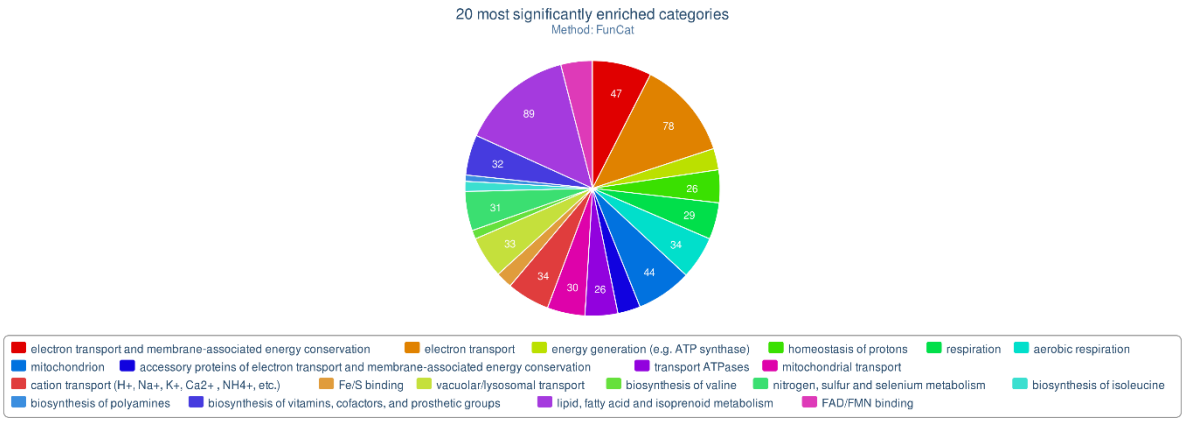

Figure 5. Differentially regulated FunCat gene categories in the *ΔMoisw2* compared to the background strain *Ku80*. (**A**) Enriched upregulated genes in the mutant; Secondary metabolism, DNA-binding, and genes for DNA-related activities and synthesis (growth). (**B**) Enriched downregulated genes in the mutant; Mitochondrial activities like electron transport and mitochondrial biosynthesis.

Regulation of DNA-binding genes closest to the MoIsw2 binding site

Since 65 genes above were classified as DNA-binding and were among the enriched genes upregulated in *ΔMoisw2* (**Fig. 5A**), we counted the number of genes positioned between

these genes and the MoIsw2 binding sites for all the DNA-binding genes. The products of some of these genes could be transcription factors directly under the control of MoISW2. We found that the most upregulated DNA binding genes in the *ΔMoisw2* are physically closest to the MoIsw2 palindromic DNA binding motif site, indicating that deleting *MoISW2* gives better DNA access for the promoters of DNA-binding genes situated close to the MoIsw2 palindromic DNA binding motif site (**Fig. 6**).

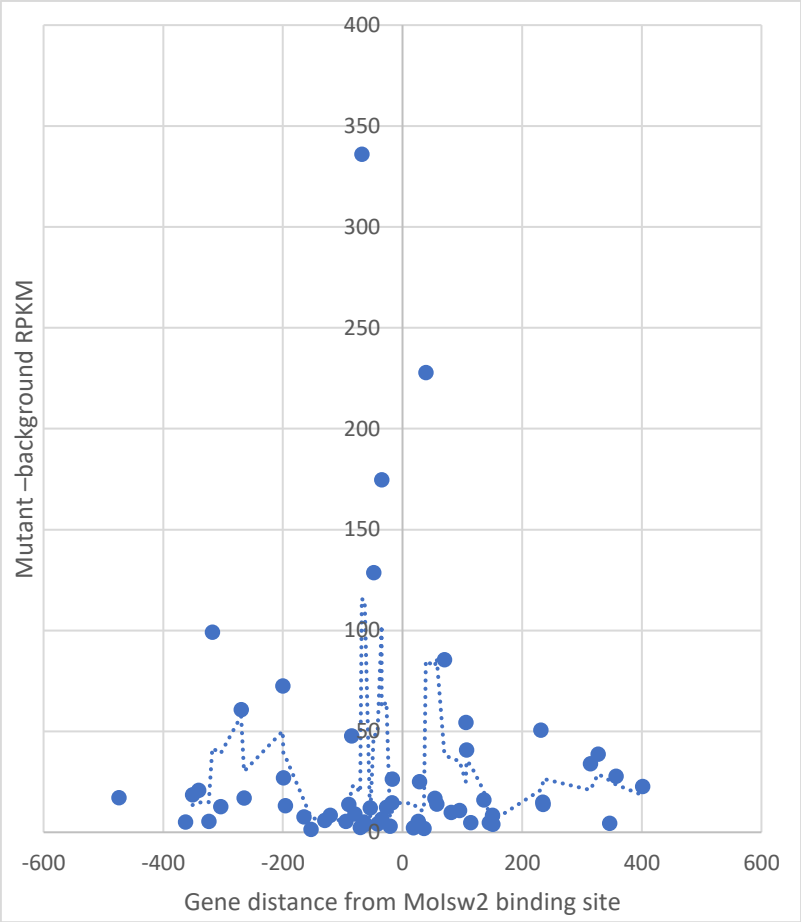

Figure 6. The enriched, most differentially regulated DNA-binding genes in *ΔMoisw2* mutation and the background strain *Ku80* are physically close to the MoISW2 palindromic DNA binding motif site. The X-axis is the plus-minus gene distance from the gene closest to the MoISW2 binding site. Also, note that there is a pattern in their regulation at different distances from the binding sites. There are 4 peaks at -300 to 200, -70 to -30, 30 to 100, and 240 to 400. The dotted line shows 3 points moving average to highlight this.

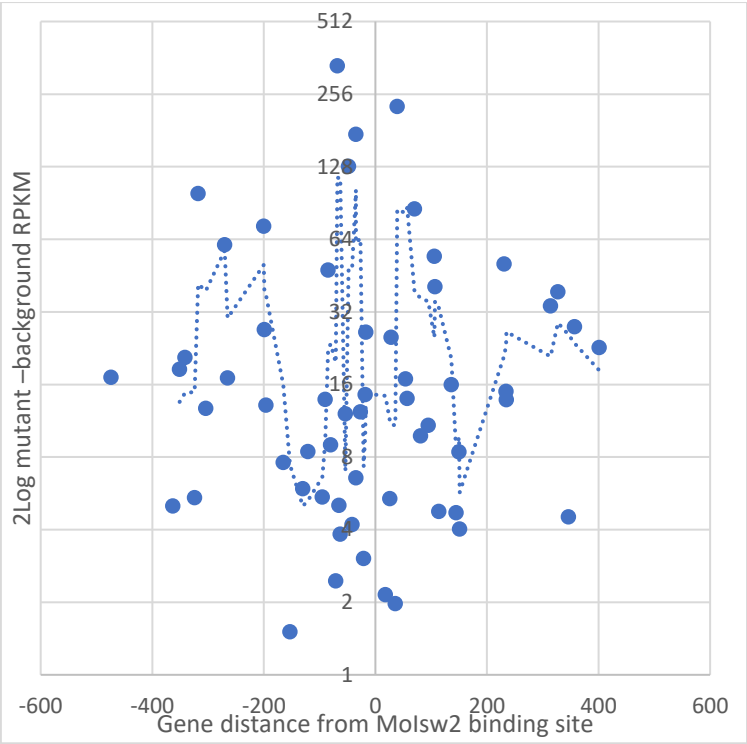

Figure S3. Same as **Fig. 6** but with 2Log Y-axis to better show that the expression of the DNA binding genes around the MoIsw2 DNA binding site has changed with the *DMoisw2* mutation. There are in principle 4 peaks at -300 to 200, -70 to -30, 30 to 100, and 240 to 400. The dotted line shows 3 points moving average to highlight this.

Table 2. Genes close to the MoIsw2 binding motif and most upregulated in *ΔMoisw2* compared to the background Ku80-strain with annotation from NCBI

MGG_02762	MGG_02762. ATP-dependent RNA helicase DED1; Belongs to the DEAD box helicase family
MGG_06470	MGG_06470, DNA repair helicase RAD25 (835 aa).
MGG_05948	MGG_05948 zinc knuckle domain-containing protein. This domain is a zinc-binding domain of the form CxxCxxxGHxxxxC from various species. It is found in the MPE1 protein from Saccharomyces cerevisiae which is a component of the cleavage and polyadenylation factor (CPF) complex important for polyadenylation-dependent pre-mRNA 3'-end formation
MGG_01990	b-ZIP transcription factor IDI-4 (induces autophagic cell death in *Podospora*)
MGG_02429	KOG4062 6-O-methylguanine-DNA methyltransferase MGMT/MGT1, involved in DNA repair Replication, recombination and repair https://jgi-myco-web-4.jgi.doe.gov/annotator/servlet/jgi.annotation.Annotation?pDb=Lasov1&pStateVar=View&pProteinId=680852&pViewType=protein
MGG_04428	Zinc finger transcription factor ace1
MGG_05995	MGG_05995, Magnaporthe oryzae 70-15 hypothetical protein (244 aa), translin family protein, Translin family (PF01997). If Translin here is a review about that https://link.springer.com/article/10.1007/s12038-019-9947-6
MGG_04429	ATP-dependent DNA helicase MPH1; ATP-dependent DNA helicase is involved in DNA damage repair by homologous recombination and genome maintenance.

Of the DNA-binding genes most suppressed by MoIsw2 activity and closest to the MoISW2 binding site, only two encode conventional TFs; the others are mainly involved in DNA repair (**Table 2**) needed for DNA synthesis and growth.

To get further information about the genes MoIsw2 nucleosome interactions directly can regulate, we investigated which genes were situated +8/-8 genes from the MoISW2 binding sites

(**Supplemental Data S4**) in the *M. oryzae* genome using FunCat classification. In the background possessing MoIsw2, these genes are more likely to be regulated (positive or negative). These genes can be expected to be most influenced by MoIsw2 chromatin-modifying activities. Interestingly, significantly enriched genes that are physically close to the MoIsw2 binding sites are gene categories indicative of interaction with the abiotic and biotic environment, while significantly depleted genes are related to DNA synthesis and growth. The depleted genes are, in principle, indicative of housekeeping. Thus, combined with the above, it appears that MoISW2 is a switch between growth (DNA synthesis) and interaction with the environment.

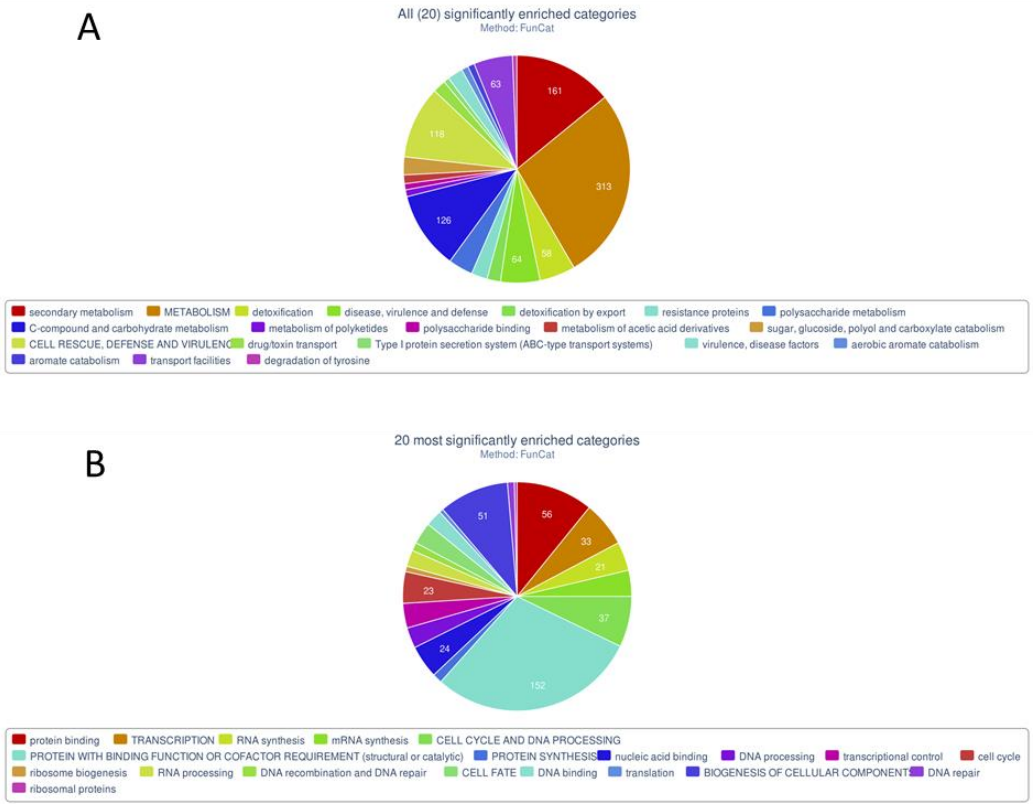

Figure 7. Significantly enriched categories (**A**) are abiotic and biotic interaction-related categories for the genes closest (8+/- 8 genes) to the MoIsw2 binding site. Significantly depleted categories (**B**) are growth-related protein and DNA synthesis-related genes.

MoIsw2 is likely involved in the regulation of core secondary metabolism genes

Interactions with the environment (biotic and abiotic) and secondary metabolism are two categories that, together with the regulation of avirulence genes and closeness to transposons, could indicate that *MoISW2* is instrumental in creating Non-Conserved Regions (NCRs) in *M. oryzae*. These gene categories positioning in NCRs have been characterized in *Fusarium. graminearum* compared to conserved regions containing housekeeping genes (Zhao et al., 2014). To investigate the positioning of secondary metabolite genes, we used the Anti-SMASH website and searched the complete MoDNA sequence for core secondary metabolite genes, so we are not dependent on previous annotations from the literature. We found 54 core secondary metabolite genes (**Supplemental Data 6**). Of these genes, 19 are positioned +8/- 8 genes from the MoIsw2 binding sites, and 25 are within

the double-distance from the binding site. Using the Fisher exact test (**Table S1**) and testing against random distribution, the P-value for the null hypothesis that the distribution is random is 2.18E-08 for the 19 genes closest to the MoIsw2 binding site and 1.93E-08 for the double gene distance from the binding site. In other words, there is a highly significant overrepresentation of secondary metabolite genes close to the MoIsw2 palindromic DNA binding motif site. Most of the 19 closest genes are also differentially regulated by MoIsw2, indicating that MoIsw2 seems to regulate their expression (**Fig. 8**) actively.

Table S1 Input for Fisher's Exact

	+8/-8genes from MoISW2 DNA binding		Double gene distance MoIsw2 DNA binding	
	Total	Sec met genes	Total	Sec met genes
In selection	951	19	1902	25
Not in selection	12233	35	11282	29

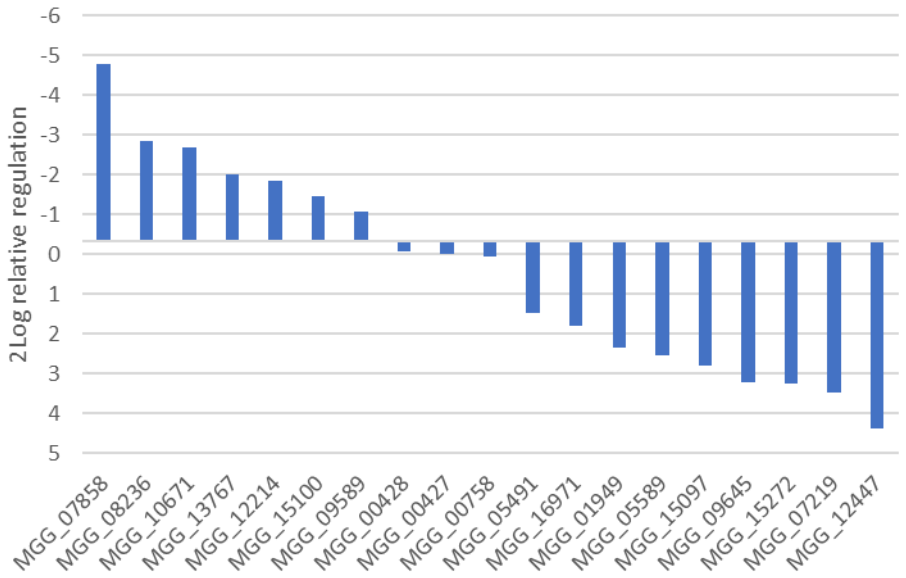

Figure 8. Core secondary metabolite genes according to an AntiSmash search of the whole genome (**Supplementary data 2**, (magnaporthe_oryzae_70-15_8_genes.zip) file containing the search output as a Zipped website unzip to a new folder to a new folder and run the index-file). Negative values show upregulation in the *Ku80* background (regulated by MoIsw2) compared to *ΔMoisw2*, while positive values show downregulation in *Ku80* compared to *ΔMoisw2.*

MoIsw2 binding to DNA sequences closest to or inside genes

We now turn back to the rest of the ChIP-seq data. We have above shown that genes under *MoISW2* control that are more expressed in the background *Ku80* strain compared to the *ΔMoisw2* strain are enriched for gene classes characteristic for secondary metabolism and biomass growth (anabolism) (**Fig. 5A**), while the downregulated genes in the mutant are genes connected to aerobic metabolism and stress (**Fig. 5A**).

In the MoIsw2 ChIP-seq data, we investigated the FunCat classification of all genes with sequence hits. First, we removed double hits not to count the same gene twice. We then investigated the list of genes closest to the MoIsw2 palindromic DNA binding motif site. These genes should be targeted by MoIsw2 and might be under positive or negative control from MoIsw2. According to the previous analysis, they should not belong to growth (anabolism) but be genes active when oxygen is consumed and the substrates oxidized (catabolism) (Klevecz et al., 2004; Machné and Murray, 2012). In addition, the binding sequences close to avirulence genes and retrotransposons, so their regulation can shift depending on retrotransposon transpositions. Since ChIP-seq only shows potential binding to DNA *in vivo,* we cannot say if these genes are up or downregulated, only that regulation influenced by MoIsw2 can occur. Genes hits closest to the MoIsw2 palindromic DNA binding motif site are mainly enriched for secondary metabolite genes and other gene classes essential for biotic interactions (**Fig. 9A**), while specific gene categories for biomass growth and housekeeping (anabolism) are depleted (**Fig. 9B**).

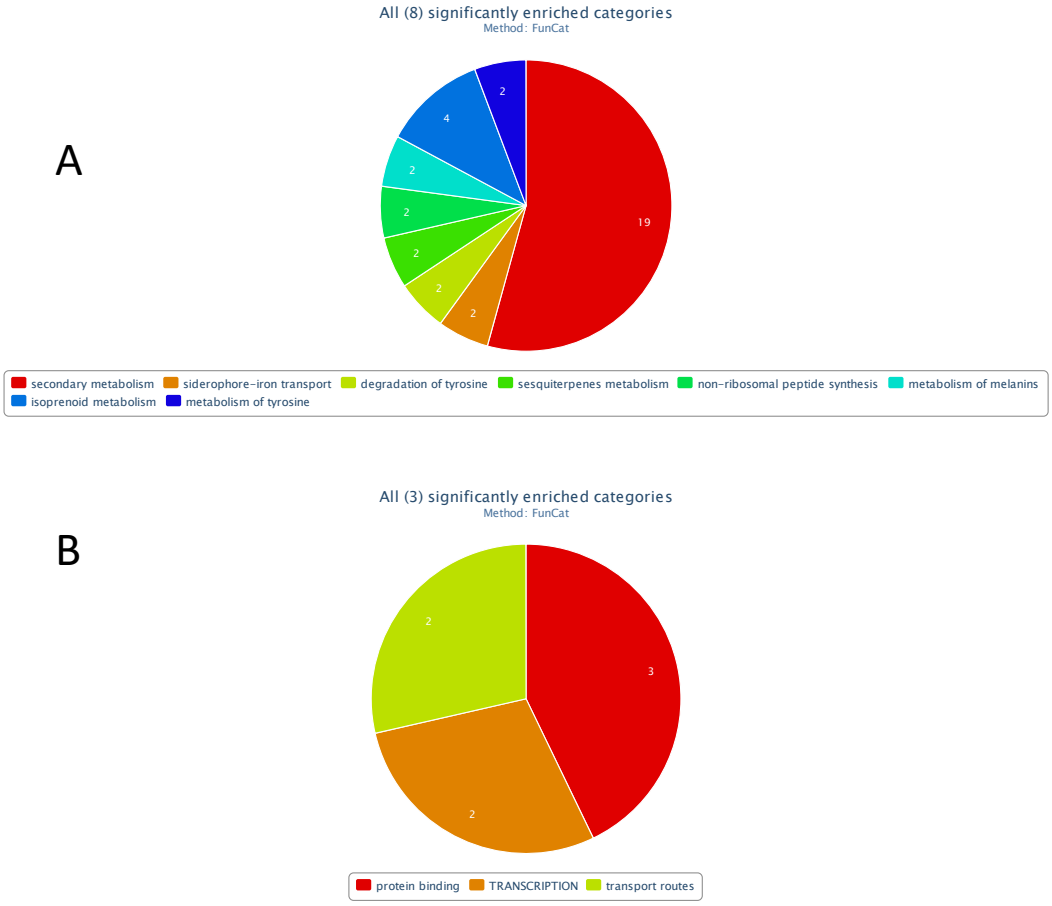

Figure 9. FunCat classification of genes closest to MoIsw2 ChIP-seq binding that also has the MoIsw2 binding palindromic motif. (**A**) Enriched classes of genes, and (**B**) depleted classes of genes.

Genes with MoISW2 binding their promoter, or in their exons, or introns are other genes likely regulated by MoIsw2 nucleosome positioning activity during anabolism/catabolism shifts. These genes are many more than those close to MoIsw2 palindromic DNA motif sites, and we detect more gene classes (**Fig. 10A**), including detoxification, signaling (cyclic nucleotide-binding), disease, and defense as classes important in biotic and abiotic interactions with the environments. Depleted are again gene classes characteristic for anabolism (biomass growth) (**Fig. 10B**)

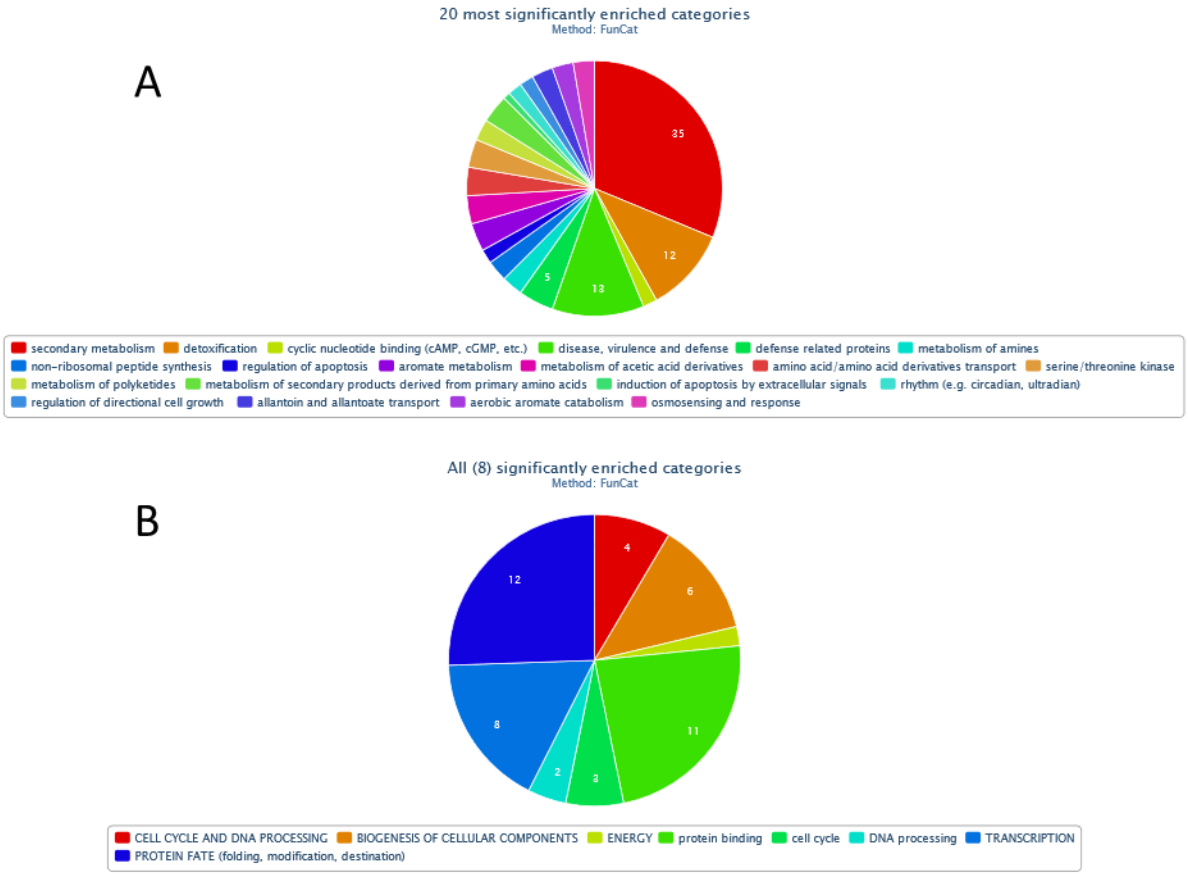

Figure 10. FunCat classifications of genes with ChIP-seq MoIsw2 binding to their DNA sequences (excluding the palindromic motif hits in **Fig. 9**). (**A**) Enriched classes of genes and (**B**) depleted classes of genes.

Finally, as shown in **Fig. 11**, the genes closest to ChIP-seq hits in intergenic regions, not containing the MoIsw2 palindromic DNA binding motif site, are again genes enriched for secondary metabolite genes and genes involved in abiotic and biotic interactions (**Fig. 11A**). In contrast, genes needed for biomass growth are again depleted (**Fig. 11B**).

A

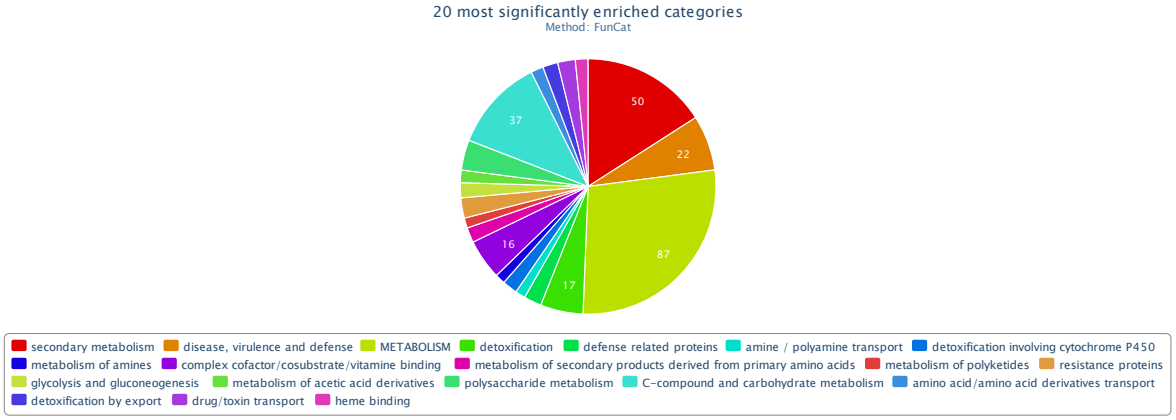

B

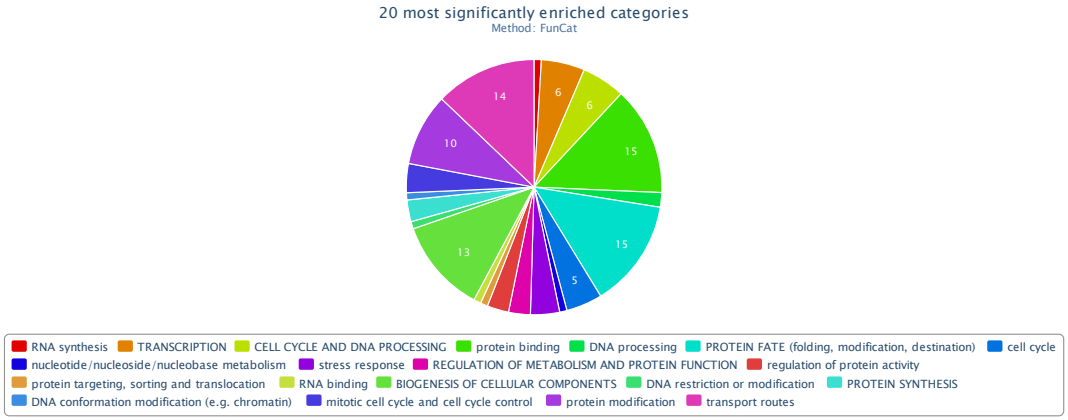

Figure 11. FunCat classifications of genes closest to intergenic hits (excluding the palindromic motif hits) for MoIsw2 binding. (**A**) Enriched classes of genes and (**B**) depleted classes of genes

Discussion

The yeast Isw1 and Isw2 interactions with His4 are very transient (approximately 200 and 80 bindings per minute, respectively) and need a continuous ATP supply (Tsukiyama et al., 1999). Thus our attempts to detect MoIsw2 interaction with MoHis4 using the yeast two-hybrid method were not likely to give positive results. Isw1 translocate nucleosomes away from other nucleosomes, while Isw2 does the same towards the center of DNA pieces and towards other nucleosomes *in vitro,* with the nucleosomes bound to relatively short DNA pieces (Kagalwala et al., 2004; Zofall et al., 2004). It does so also *in vivo* where it was found that Isw2 is mainly involved in targeted silencing of DNA around the ISW2 DNA binding site (Fazzio et al., 2005), as we also find (**Fig. 3,6, Table 1**). Taken together, this silencing of genes closest to the DNA-binding site should be very ATP-dependent and dependent on the competition for ATP in the cytoplasm and nucleus shared compartment of free diffusion for small molecules.

ATP generation from fermentation is much faster than from oxidative phosphorylation when glucose is available. In yeast, growth is also characterized by DNA replication, mainly without mitochondrial oxidative activity (aerobic glycolysis), most probably to protect DNA from mutations (Klevecz et al., 2004). In *M. oryzae* MoIsw2 could thus be an ATP regulated switch (Machné and Murray, 2012) between fast aerobic glycolysis,

DNA-synthesis growth and quality control,and slower but more high ATP yield efficient oxidative phosphorylation growth, oxidative defenses, and interaction with the abiotic and biotic environment that makes up the *M. oryzae* ecological niche. We found that genes upregulated in the *ΔMoisw2* mutant are involved in fast growth and DNA-synthesis, and also genes necessary for DNA quality control while downregulated genes in the mutant were those involved in oxidative phosphorylation, stress management, and secondary metabolite biosynthesis (**Fig. 5** and **Table 2**). As expected, the genes closest to the two central nucleosomes to the binding site should be downregulated in the background *Ku80* (Donovan et al., 2021), and when MoIsw2 is deleted, such genes should be upregulated. We could also note that downregulation in the background *Ku80* depended on the distance from the ISW2 binding site (**Fig. 2**). Outside this central downregulation of DNA synthesis related genes and two TFs close to the ISW2 binding sites (**Fig. 6**), genes are expected to become more easily regulated since the ISW2 positioning of two nucleosomes close gives more sliding space of surrounding nucleosomes and thus the possibility for regulation (Donovan et al., 2021). The 16 genes closest to the predicted MoIsw2 palindromic DNA binding motif sites are expected to be most affected by MoIsw2 local nucleosome condensation. These are genes involved in responding to environmental cues (secondary metabolite production, oxidative stress response), further strengthening the general observation about genes regulated in the mutant (**Fig. 2**).

Our observations suggest that the *M. oryzae* genome is divided into genes needed for interaction with the environment similarly surrounded by house-keeping genes as described for the non-conserved regions in *Fusarium graminearu*m where these types of genes are overrepresented (Zhao et al., 2014). One of the most potential DNA-binding sites for the MoISW2 is a palindromic motif giving instability to the genome at this site (Ganapathiraju et al., 2020; Svetec Miklenić and Svetec, 2021) and characteristic of motifs for retrotransposons situated close to stress-related genes and avirulence genes (plant pathogen effectors with a difference in resistance against by cultivars, thus the cause of avirulence against these cultivars)(Yoshida et al., 2016). The authors also found that a gene linkage to transposons is connected with elevated mutation rates. Different mutation rates or mutation bias of genes as a new concept have recently been described for the plant *Arabidopsis thaliana* (Monroe et al., 2022). Genes with higher mutation rates are involved in biotic and abiotic interactions, and the gene found with the highest mutation rate was a gene responding to chitin present in fungi and insects (Monroe et al., 2022). Our results show changes in the regulation of the avirulence genes between two *M. oryzae* strains with different pathogenicity to different rice cultivars (**Table 2**). Also, we could not detect any expression for some putative avirulence genes close to the MoIsw2 binding sites indicating that those genes are potential pseudogenes in these strains. That might indicate a retrotransposon-aided genetic evolution of inherited epigenetic changes to regulation in reactions to the environment (resistance of the plant cultivar). A regulation that can be genetically fixed, first through loss of possible regulation (making genes into pseudogenes), and much later complete gene loss or break-up of the potential pseudogenes so they cannot be easily recognized as genes.

Potential pseudogenes close to retrotransposons were also found for stress-induced retrotransposon activities resulting in a "biased" faster evolution (Chadha and Sharma, 2014). The loss of *ISW2* function in a unicellular Eukaryote or the early stages of fungal growth from a spore should make it unfit for survival in a natural environment. Our results indicate that *MoISW2* regulates a switch between fast glycolytic growth and slower aerobic stress characterized growth, coping with abiotic and biotic stresses, or in other words, niche fitness. However, fast glycolytic growth could result in fast uncontrolled cell

growth in a long-lived multicellular organism since ATP and glucose can be received from surrounding cells and other tissues through the blood circulation.

Mutations of the genes *SMARKA2* or *SMARKA4* that encode BRM and BRG1 proteins that are orthologues of fungal Swi2/Snf2 involved in nucleosome positioning in a way that has similarities to the nucleosome movements Isw2 cause (Reisman et al., 2009; Mittal and Roberts, 2020). In many cancer types, *SMARKA2* or *SMARKA4* are mutated (Reisman et al., 2009; Hasan and Ahuja, 2019; Mittal and Roberts, 2020). The human gene encoding an orthologue protein to MoIsw2 is *SMARCA1*, and mutations in this gene can cause some cancers (Ye et al., 2009). However, a knockdown of *SMARCA1*s activities in breast cancer cell lines causes increased apoptosis-independent DNA damage, killing cancer cells, although not all breast cancer lines are dependent on its expression for survival (Ye et al., 2009).

A general shift to aerobic glycolysis and fast upregulation (within a few hours) of innate immunity-related genes associated with tissue inflammation is characteristic of fast defense against microbes through fast iron uptake, antimicrobial peptide production, and other responses needing rapid translational responses, as shown for *Fusarium graminearum* is general for eukaryotes (Ipcho et al., 2016). Such fast upregulated innate immune response in plants can be inhibited by fungal immune inhibitors acting on translation like trichothecenes the same fungus produce (Toyotome and Kamei, 2021), most likely to attenuate immune responses in the plants it infects. In consequence with this scenario, genes involved in RNA synthesis and RNA processing were upregulated in the *ΔMoisw2* mutant (**Fig. 5A**), although the protein synthesis machinery is part of the general housekeeping and is further away from the MoIsw2 DNA palindromic binding motif (**Fig. 7).** The latter point to a division of the *M. oryzae* genome into regions responsive to changes in the environment close to the MoIsw2 palindromic DNA binding motif site and regions with mainly housekeeping genes between these binding sites in a way slightly similar to what is described for *F. graminearum* non-conserved regions and conserved regions (Zhao et al., 2014) and what is also found for mutation bias in *A. thaliana* (Monroe et al., 2022). The high-mutation probability genes found in *A. thaliana* were mainly genes necessary for recognizing and responding to abiotic and biotic challenges (Monroe et al., 2022). The latter indicates that evolution to better fit the niche (evolution of new species and strains) proceeds faster than random mutation in the whole genome alone, followed by selection (Monroe et al., 2022).

MoISW2 is possibly taking part in a mechanism aiding both mutation bias and adaptation to new circumstances whose combined activities lead to natural adaptation-directed fast evolution (NADFE), a bit similar to artificial adaptation-directed fast evolution that can be performed in a laboratory (Packer and Liu, 2015). Since transposon MoIsw2 palindromic DNA binding seems necessary for binding to these palindromic sites, stress-activated transposon activity known for creating genomic instability can then, together with the MoIsw2 activity, create a new adaptive regulatory landscape (Chadha and Sharma, 2014) that can be stabilized relatively quickly and lead to a sort of mutation bias (Monroe et al., 2022). It also would, in addition, be one mechanism sought after for a Lamarckian-Darwinian synthesis to help explain the fast evolution of new traits requiring many combined mutations that cannot be reconciled within Darwinian evolution based only on random mutations creating variation and sexual recombination with natural selection favoring the better fitted (Bard, 2011). The chance of multiple mutations that together can become positive is theoretically much more likely with NADFE aided by mutation bias (Monroe et al., 2022). *ISW2*

activities in eukaryotes could thus be one of the needed mechanisms to reconcile Lamarckian evolution with Darwinian evolution to bring about both the observed direction and the needed speed of evolution of specific traits when new niches become available or there are drastic niche changes (Bard, 2011).

As a consequence of the present research, the effect of exposing *M. oryzae* strains to different MoIsw2 activities and retrotransposon activities on the rate of genetic adaptation to a shift in rice cultivar is a possible future topic that could be exploited to understand how the pathogen adapts to different resistant cultivar and break plant resistance. Searching for potential agrochemicals to manipulate *MoISW2* activities is tempting since *MoISW2* is crucial for plant pathogenicity, although MoIsw2's close resemblance to mammalian proteins with the same function indicates that such chemicals are likely affecting mammals and might be cancerogenic to humans. Finally, we found 2 *MoHIS4* genes predicted to encode for identical proteins but differently regulated (**Fig. 1**), and it seems like *M. oryzae* needs both genes. This fact is of interest since His4 in the nucleosomes is what MoIsw2 is supposed to interact with (Tsukiyama et al., 1999) and are examples of genes with the highest degree of purifying evolution (Piontkivska et al., 2002). We have thus started new research into the roles and regulation of these two *MoHIS4* genes and how their regulations shift with growth conditions. Their predicted identical amino acid sequences indicate that they are evolutionarily constrained to differ only by synonymous mutations.

Materials and Methods

Fungal strains and media

Magnaporthe oryzae (B. Couch) anamorph of the teleomorph *Pyricularia oryzae* (Cavara) was the fungus used. The *MoISW2-GFP* complement strain derived from the *ΔMoisw2* strain in the background strain *Ku80* has previously been described (Li et al., 2021). For both ChIP-seq and RNAseq, the strains used were grown and harvested in the same way. For ChIP-seq MoISW2-GFP and Ku80 were used, and for RNAseq *ΔMoisw2* and *Ku80* were used. The strains were grown on CM2 solid medium.

Complete medium 2 (CM2) all quantities L^{-1}: 20X Mineral salts solution 50mL, 1000X Trace element solution 1mL, 1000X vitamin solution 1mL, D-glucose 10g, peptone 2g, casamino acid 1g, yeast extract 1g, pH 6.5. For agar medium add 15g agar.

20×Mineral salts solution(1000mL): NaNO3 120g，KCl 10.4g，MgSO4 7H2O 10.4g，KH2PO4 30.4g

1000X Vitamin solution (100mL) Biotin 0.01g, Pyridoxin 0.01g, Thiamine 0.01g, Riboflavin 0.01g, PABA (p-aminobenzoic acid) 0.01g, Nicotinic acid 0.01g.

1000X Trace element (100mL): $ZnSO_4$ $7H_2O$ 2.2g, H_3BO_3 1.1g $MnCl_2$ $4H_2O$ 0.5g, $FeSO_4$ $7H_2O$ 0.5g $CoCl_2$ $6H_2O$ 0.17g, $CuSO_4$ $5H_2O$, Na_2MoO_4 $5H_2O$ 0.15g, EDTA 4Na 5g.

The plates were incubated 4-5 days at 28°C with alternating light-dark cycles (12/12). Mycelial disks (15-20) were punched out using a cork puncher at the colony's edge. The disks were then transferred to 100 ml CM2 liquid medium and cultured for another 48h with shaking (160 RPM, Constant temperature culture oscillator, ZHWY-2102C, Shanghai Zhicheng Analytical Instrument

Manufacturing Co., Ltd.). The obtained biomass was filtered using Miracloth, frozen in liquid nitrogen, and sent to the company on dry ice.

ChIP-seq and RNA-seq as well as RNA-seq.

Both these techniques were carried out by the company Wuhan IGENEBOOK Biotechnology Co.,Ltd, China, according to their method descriptions **(Supplemental Company Methods file**). The last steps about finding motifs and finding enriched gene classes were carried out differently and these steps not used are marked in the two method files.

Additional software and add-ins

Addins for MS Excel. The **Fisher Exact** add-in for MS Excel was downloaded from http://www.obertfamily.com/software/fisherexact.html. **Excel solver** is usually part of the MS Excel but must be activated in settings.

Freeware: We used the freeware PAST (Hammer et al., 2001) version 4.08 (released November 2021) for Reduced Major Axis (RMA) regression analysis to handle errors in both the x and y variables. A simple to use but powerful freeware program is available from the University of Oslo, Natural History Museum **https://www.nhm.uio.no/english/research/infrastructure/past/.** For simplicity, the data was handled and entered in MS Excel and then copy-pasted into PAST for analysis. The resulting plots were exported from PAST as SVG ector graphic files to be later translated into other vector graphic file formats.

Websites used for analyses and getting necessary additional data

NCBI: **https://www.ncbi.nlm.nih.gov/** (sequence downloads, blasts, annotations including domain annotations)

BROAD: **ftp://ftp.broadinstitute.org** (download of gene order on supercontigs for the 70-15 strain, 1000 upstream DNA sequences for use in MEME)

MEME: https://meme-suite.org/meme/ (use of MEME and FIMO). (Bailey et al., 2015).

See the supplemental file for MEME settings and complete results (Supplemental Data 2). MEME motif 2 was the one with the most hits and was investigated in detail. This motif2 was used for TOMTOM by using the direct link to TOMTOM using the link from the MEME result, for results see the supplemental file (Supplemental Data 3).

FungiFun2 https://elbe.hki-jena.de/fungifun/fungifun.php (Priebe et al., 2015)

Species**:** *Magnaporthe grisea* 70-15 (synonym for *M. oryzae* 70-15).

Classification ontology: FunCat (contains relevant categories for plant pathogens)

Input IDs: For *M. oryzae* 70-15 the MGG_ codes has to be used.

Advanced settings used**:** Significance level; 0.05. Significance test; Fisher's exact test. Test for; Enrichment or Depletion. Adjustment method; No adjustment. Annotation type, Select also indirectly annotated categories.

These settings using No adjustment were used since the purpose was not to get super reliable enriched or depleted categories but to compare several FungiFun runs with different Gene ID sets.

antiSMASH

The complete DNA sequence was downloaded from BROAD. That was then submitted to antiSMASH (Blin et al., 2021) fungal version **https://fungismash.secondarymetabolites.org/#!/start** and run with default parameter settings to find the primary genes predicted to be involved in producing secondary metabolites.

Acknowledgments

Professor Daniel J. Ebbole, Texas A&M University, USA, is thanked since he pointed us to the Supercontig sorted gene file for the strain 70-15 that could be downloaded from the BROAD institute. This file was necessary for the present work. The National Science Foundation China financially supported this research (NSFC31871914).

References

Bailey, T.L., Johnson, J., Grant, C.E., Noble, W.S., 2015. The MEME Suite. Nucleic Acids Res 43, W39–W49. https://doi.org/10.1093/nar/gkv416

Bard, J.B., 2011. The next evolutionary synthesis: from Lamarck and Darwin to genomic variation and systems biology. Cell Commun Signal 9, 30. https://doi.org/10.1186/1478-811X-9-30

Blin, K., Shaw, S., Kloosterman, A.M., Charlop-Powers, Z., van Wezel, G.P., Medema, M.H., Weber, T., 2021. antiSMASH 6.0: improving cluster detection and comparison capabilities. Nucleic Acids Research 49, W29–W35. https://doi.org/10.1093/nar/gkab335

Chadha, S., Sharma, M., 2014. Transposable Elements as Stress Adaptive Capacitors Induce Genomic Instability in Fungal Pathogen Magnaporthe oryzae. PLoS ONE 9, e94415. https://doi.org/10.1371/journal.pone.0094415

Cheetham, S.W., Faulkner, G.J., Dinger, M.E., 2020. Overcoming challenges and dogmas to understand the functions of pseudogenes. Nat Rev Genet 21, 191–201. https://doi.org/10.1038/s41576-019-0196-1

Chereji, R.V., Ramachandran, S., Bryson, T.D., Henikoff, S., 2018. Precise genome-wide mapping of single nucleosomes and linkers in vivo. Genome Biol 19, 19. https://doi.org/10.1186/s13059-018-1398-0

Collemare, J., Pianfetti, M., Houlle, A., Morin, D., Camborde, L., Gagey, M., Barbisan, C., Fudal, I., Lebrun, M., Böhnert, H.U., 2008. *Magnaporthe grisea* avirulence gene *ACE1* belongs to an infection-specific gene cluster involved in secondary metabolism. New Phytologist 179, 196–208. https://doi.org/10.1111/j.1469-8137.2008.02459.x

Cutter, A.R., Hayes, J.J., 2015. A brief review of nucleosome structure. FEBS Letters 589, 2914–2922. https://doi.org/10.1016/j.febslet.2015.05.016

Dang, W., Sutphin, G.L., Dorsey, J.A., Otte, G.L., Cao, K., Perry, R.M., Wanat, J.J., Saviolaki, D., Murakami, C.J., Tsuchiyama, S., Robison, B., Gregory, B.D., Vermeulen, M., Shiekhattar, R., Johnson, F.B., Kennedy, B.K., Kaeberlein, M., Berger, S.L., 2014. Inactivation of Yeast Isw2 Chromatin Remodeling Enzyme Mimics Longevity Effect of Calorie Restriction via Induction of Genotoxic Stress Response. Cell Metabolism 19, 952–966. https://doi.org/10.1016/j.cmet.2014.04.004

Dioh, W., Tharreau, D., Notteghem, J.L., Orbach, M., Lebrun, M.-H., 2000. Mapping of Avirulence Genes in the Rice Blast Fungus, *Magnaporthe grisea* , with RFLP and RAPD Markers. MPMI 13, 217–227. https://doi.org/10.1094/MPMI.2000.13.2.217

Donovan, D.A., Crandall, J.G., Truong, V.N., Vaaler, A.L., Bailey, T.B., Dinwiddie, D., Banks, O.G., McKnight, L.E., McKnight, J.N., 2021. Basis of specificity for a conserved and promiscuous chromatin remodeling protein. eLife 10, e64061. https://doi.org/10.7554/eLife.64061

Fazzio, T.G., Gelbart, M.E., Tsukiyama, T., 2005. Two Distinct Mechanisms of Chromatin Interaction by the Isw2 Chromatin Remodeling Complex In Vivo. Mol Cell Biol 25, 9165–9174. https://doi.org/10.1128/MCB.25.21.9165-9174.2005

Ganapathiraju, M.K., Subramanian, S., Chaparala, S., Karunakaran, K.B., 2020. A reference catalog of DNA palindromes in the human genome and their variations in 1000 Genomes. Hum Genome Var 7, 40. https://doi.org/10.1038/s41439-020-00127-5

Hammer, O., Harper, D.A.T., Ryan, P.D., 2001. PAST: Paleontological Statistics Software Package for Education and Data Analysis 4, 9.

Hasan, N., Ahuja, N., 2019. The Emerging Roles of ATP-Dependent Chromatin Remodeling Complexes in Pancreatic Cancer. Cancers 11, 1859. https://doi.org/10.3390/cancers11121859

Hota, S.K., Bartholomew, B., 2011. Diversity of operation in ATP-dependent chromatin remodelers. Biochimica et Biophysica Acta (BBA) - Gene Regulatory Mechanisms 1809, 476–487. https://doi.org/10.1016/j.bbagrm.2011.05.007

Huang, L., Li, X., Dong, L., Wang, B., Pan, L., 2021. Profiling of chromatin accessibility identifies transcription factor binding sites across the genome of Aspergillus species. BMC Biol 19, 189. https://doi.org/10.1186/s12915-021-01114-0

Ipcho, S., Sundelin, T., Erbs, G., Kistler, H.C., Newman, M.-A., Olsson, S., 2016. Fungal innate immunity induced by bacterial microbe-associated molecular patterns (MAMPs). G3 6, 1585–1595. https://doi.org/10.1534/g3.116.027987

Kagalwala, M.N., Glaus, B.J., Dang, W., Zofall, M., Bartholomew, B., 2004. Topography of the ISW2–nucleosome complex: insights into nucleosome spacing and chromatin remodeling. EMBO J 23, 2092–2104. https://doi.org/10.1038/sj.emboj.7600220

Klevecz, R.R., Bolen, J., Forrest, G., Murray, D.B., 2004. A genomewide oscillation in transcription gates DNA replication and cell cycle. Proceedings of the National Academy of Sciences 101, 1200–1205. https://doi.org/10.1073/pnas.0306490101

Li, Y., Zheng, X., Pei, M., Chen, M., Zhang, S., Liang, C., Gao, L., Huang, P., Olsson, S., 2021. Identification and characterization of 19 predicted Myb-family DNA binding proteins in *Magnaporthe oryzae* concerning growth, conidiation, and pathogenicity (preprint). BioRxiv. https://doi.org/10.1101/2021.12.28.474317

Linheiro, R.S., Bergman, C.M., 2008. Testing the palindromic target site model for DNA transposon insertion using the Drosophila melanogaster P-element. Nucleic Acids Research 36, 6199–6208. https://doi.org/10.1093/nar/gkn563

Machné, R., Murray, D.B., 2012. The Yin and Yang of Yeast Transcription: Elements of a Global Feedback System between Metabolism and Chromatin. PLoS ONE 7, e37906. https://doi.org/10.1371/journal.pone.0037906

Mittal, P., Roberts, C.W.M., 2020. The SWI/SNF complex in cancer — biology, biomarkers and therapy. Nat Rev Clin Oncol 17, 435–448. https://doi.org/10.1038/s41571-020-0357-3

Monroe, J.G., Srikant, T., Carbonell-Bejerano, P., Becker, C., Lensink, M., Exposito-Alonso, M., Klein, M., Hildebrandt, J., Neumann, M., Kliebenstein, D., Weng, M.-L., Imbert, E., Ågren, J., Rutter, M.T., Fenster, C.B., Weigel, D., 2022. Mutation bias reflects natural selection in Arabidopsis thaliana. Nature 602, 101–105. https://doi.org/10.1038/s41586-021-04269-6

Packer, M.S., Liu, D.R., 2015. Methods for the directed evolution of proteins. Nat Rev Genet 16, 379–394. https://doi.org/10.1038/nrg3927

Piontkivska, H., Rooney, A.P., Nei, M., 2002. Purifying Selection and Birth-and-death Evolution in the Histone H4 Gene Family. Molecular Biology and Evolution 19, 689–697. https://doi.org/10.1093/oxfordjournals.molbev.a004127

Priebe, S., Kreisel, C., Horn, F., Guthke, R., Linde, J., 2015. FungiFun2: a comprehensive online resource for systematic analysis of gene lists from fungal species. Bioinformatics 31, 445–446. https://doi.org/10.1093/bioinformatics/btu627

Reisman, D., Glaros, S., Thompson, E.A., 2009. The SWI/SNF complex and cancer. Oncogene 28, 1653–1668. https://doi.org/10.1038/onc.2009.4

Serrano, L., Vazquez, B.N., Tischfield, J., 2013. Chromatin structure, pluripotency and differentiation. Exp Biol Med (Maywood) 238, 259–270. https://doi.org/10.1177/1535370213480718

Song, Z., Bakeer, W., Marshall, J.W., Yakasai, A.A., Khalid, R.M., Collemare, J., Skellam, E., Tharreau, D., Lebrun, M.-H., Lazarus, C.M., Bailey, A.M., Simpson, T.J., Cox, R.J., 2015. Heterologous expression of the avirulence gene ACE1 from the fungal rice pathogen Magnaporthe oryzae. Chem. Sci. 6, 4837–4845. https://doi.org/10.1039/C4SC03707C

Svetec Miklenić, M., Svetec, I.K., 2021. Palindromes in DNA—A Risk for Genome Stability and Implications in Cancer. IJMS 22, 2840. https://doi.org/10.3390/ijms22062840

Toyotome, T., Kamei, K., 2021. In Vitro Assay of Translation Inhibition by Trichothecenes Using a Commercially Available System. Toxins 13, 696. https://doi.org/10.3390/toxins13100696

Tsukiyama, T., Palmer, J., Landel, C.C., Shiloach, J., Wu, C., 1999. Characterization of the Imitation Switch subfamily of ATP-dependent chromatin-remodeling factors in Saccharomyces cerevisiae. Genes & Development 13, 686–697. https://doi.org/10.1101/gad.13.6.686

van Holde, K.E., 1989. Chromatin, Springer Series in Molecular Biology. Springer New York, New York, NY. https://doi.org/10.1007/978-1-4612-3490-6

Whitehouse, I., Rando, O.J., Delrow, J., Tsukiyama, T., 2007. Chromatin remodelling at promoters suppresses antisense transcription. Nature 450, 1031–1035. https://doi.org/10.1038/nature06391

Willcockson, M.A., Healton, S.E., Weiss, C.N., Bartholdy, B.A., Botbol, Y., Mishra, L.N., Sidhwani, D.S., Wilson, T.J., Pinto, H.B., Maron, M.I., Skalina, K.A., Toro, L.N., Zhao, J., Lee, C.-H., Hou, H., Yusufova, N., Meydan, C., Osunsade, A., David, Y., Cesarman, E., Melnick, A.M., Sidoli, S., Garcia, B.A., Edelmann, W., Macian, F., Skoultchi, A.I., 2021. H1 histones control the epigenetic landscape by local chromatin compaction. Nature 589, 293–298. https://doi.org/10.1038/s41586-020-3032-z

Ye, Y., Xiao, Y., Wang, W., Wang, Q., Yearsley, K., Wani, A.A., Yan, Q., Gao, J.-X., Shetuni, B.S., Barsky, S.H., 2009. Inhibition of Expression of the Chromatin Remodeling Gene, *SNF2L* , Selectively Leads to DNA Damage, Growth Inhibition, and Cancer Cell Death. Mol Cancer Res 7, 1984–1999. https://doi.org/10.1158/1541-7786.MCR-09-0119

Yoshida, K., Saunders, D.G.O., Mitsuoka, C., Natsume, S., Kosugi, S., Saitoh, H., Inoue, Y., Chuma, I., Tosa, Y., Cano, L.M., Kamoun, S., Terauchi, R., 2016. Host specialization of the blast fungus Magnaporthe oryzae is associated with dynamic gain and loss of genes linked to transposable elements. BMC Genomics 17, 370. https://doi.org/10.1186/s12864-016-2690-6

Zhang, L., Zhang, D., Liu, D., Li, Y., Li, H., Xie, Y., Wang, Z., Hansen, B.O., Olsson, S., 2019. Conserved Eukaryotic Kinase CK2 Chaperone Intrinsically Disordered Protein Interactions. Appl Environ Microbiol 86, e02191-19, /aem/86/2/AEM.02191-19.atom. https://doi.org/10.1128/AEM.02191-19

Zhao, C., Waalwijk, C., de Wit, P.J., Tang, D., van der Lee, T., 2014. Relocation of genes generates non-conserved chromosomal segments in Fusarium graminearumthat show distinct and co-regulated gene expression patterns. BMC Genomics 15, 191. https://doi.org/10.1186/1471-2164-15-191

Zofall, M., Persinger, J., Bartholomew, B., 2004. Functional Role of Extranucleosomal DNA and the Entry Site of the Nucleosome in Chromatin Remodeling by ISW2. Mol Cell Biol 24, 10047–10057. https://doi.org/10.1128/MCB.24.22.10047-10057.2004